tvst

Retina

# Early Alterations in Inner-Retina Neural and Glial Saturated Responses in Lens-Induced Myopia

**Reynolds K. Ablordeppey[1], Rita Nieu[1], Carol R. Lin[1], and Alexandra Benavente-Perez[1]**

[1] Department of Biological and Vision Sciences, State University of New York College of Optometry, New York, NY, USA

**Correspondence:** Alexandra Benavente-Perez, Department of Biological and Vision Sciences, State University of New York College of Optometry, 33 W 42nd St., New York, NY 10036, USA. e-mail: abenavente@sunyopt.edu

**Received:** July 19, 2023
**Accepted:** March 11, 2024
**Published:** April 9, 2024

**Keywords:** electroretinography; myopia; emmetropization; photopic negative response (PhNR), inner retina

**Citation:** Ablordeppey RK, Nieu R, Lin CR, Benavente-Perez A. Early alterations in inner-retina neural and glial saturated responses in lens-induced myopia. Transl Vis Sci Technol. 2024;13(4):16, https://doi.org/10.1167/tvst.13.4.16

**Purpose:** Myopic marmosets are known to exhibit significant inner retinal thinning compared to age-matched controls. The purpose of this study was to assess inner retinal activity in marmosets with lens-induced myopia compared to age-matched controls and evaluate its relationship with induced changes in refractive state and eye growth.

**Methods:** Cycloplegic refractive error (Rx), vitreous chamber depth (VCD), and photopic full-field electroretinogram were measured in 14 marmosets treated binocularly with negative contact lenses compared to 9 untreated controls at different stages throughout the experimental period (from 74 to 369 days of age). The implicit times of the a-, b-, d-, and photopic negative response (PhNR) waves, as well as the saturated amplitude ($V_{max}$), semi-saturation constant (K), and slope (n) estimated from intensity-response functions fitted with Naka-Rushton equations were analyzed.

**Results:** Compared to controls, treated marmosets exhibited attenuated b-, d-, and PhNR waves $V_{max}$ amplitudes 7 to 14 days into treatment before compensatory changes in refraction and eye growth occurred. At later time points, when treated marmosets had developed axial myopia, the amplitudes and implicit times of the b-, d-, and PhNR waves were similar between groups. In controls, the PhNR wave saturated amplitude increased as the b + d-wave $V_{max}$ increased. This trend was absent in treated marmosets.

**Conclusions:** Marmosets induced with negative defocus exhibit early alterations in inner retinal saturated amplitudes compared to controls, prior to the development of compensatory myopia. These early ERG changes are independent of refraction and eye size and may reflect early changes in bipolar, ganglion, amacrine, or glial cell physiology prior to myopia development.

**Translational Relevance:** The early changes in retinal function identified in the negative lens-treated marmosets may serve as clinical biomarkers to help identify children at risk of developing myopia.

## Introduction

A disruption to the emmetropization process can result in a mismatch between the optical power of the eye and its axial length, leading to refractive error development.[1] Myopia is not only a refractive and visual inconvenience, it significantly increases the risk of visual impairment caused by myopic maculopathy, cataracts, and glaucoma, among others.[2]

Evidence from experimental models of myopia confirms that the regulation of eye growth is locally controlled within the retina.[3] Several retinal cells and visual processing pathways appear involved in myopia development.[4–6] Alterations in the ON and OFF pathway affect differently the normal ocular development of mice,[5,7] cats,[8] and chicks.[9] In humans, it is hypothesized that ON and OFF asymmetries may increase the risk of myopia development,[10] which is receiving considerable attention due to its involvement with retinal dopamine, a neurotransmitter critical for ocular development.[11]

Myopia development and progression can also affect the structure of the eye. Non-human primates induced with myopia exhibit a thinning of the ganglion cell complex,[12] retinal glial, and vasculature changes,[13] and a differential activation of gene transcriptomes,[14] all of which may affect retinal function. Results from

studies assessing retinal function in myopes using electroretinograms (ERGs) are mixed, but most point to an attenuation of the a-wave (cone and OFF-bipolar cells[15]) and b-wave amplitudes (ON- and OFF-cone bipolar cells[16,17]) with no changes in their implicit times.[18,19] This finding is also supported by evidence from genetic studies.[20,21]

The photopic negative response (PhNR) is the slow negative wave that follows the b-wave and generates from the inner retina: ganglion cells and glial cells in humans[22] and non-human primates,[23–25] and amacrine cells in rodents.[26] The PhNR has been used to monitor diseases such as glaucoma,[24,25] optic atrophy,[27] diabetic retinopathy,[28] and central retinal artery occlusion.[29] However, no study to date has described how myopia affects the PhNR. The present study addresses this gap by investigating the effect of myopia on inner retina neuronal and glial cell activity. To provide a comprehensive picture of the retinal processing changes occurring in myopic eyes, and because ganglion cells receive input from bipolar cells, we studied the PhNR, a-, b-, and d-waves in juvenile and adolescent primate eyes (marmosets, *Callithrix jacchus*) induced with myopia before and after refractive and ocular growth changes are evident compared to untreated animals that emmetropized normally. Studying the activity of inner retinal cells prior and during the development of myopia may lead to the identification of early biomarkers of myopia progression that could be used to guide early interventions and help provide answers to clinically relevant questions about the development of degenerative myopia.

# Methods

## Experimental Protocol

Twenty-five juvenile marmosets were measured for this study, 14 of which were treated binocularly with single-vision negative soft contact lenses to induce myopia from approximately 70 days of age for a minimum of 12 weeks and a maximum of 44 weeks ($N = 14$; 5 males [Ms] and 9 females [Fs]). Nine marmosets were untreated controls ($N = 9$; 7 Ms and 2 Fs). Sample size calculations were obtained using a power analysis ($\alpha$-level = 0.05 and power = 80%) with preliminary data obtained from our early protocol development phase. The myopia-inducing lens rearing paradigm and outcome measurements used in this study have been previously described.[30,31] In summary, marmosets were reared on a 9-hour light (approximately 700 lux)/15-hour dark cycle at 22°C with 60% relative humidity and free access to water and food throughout the duration of the experiment. Soft contact lenses (methafilcon A: 58% water content and 21 Dk/t; Capricornia Contact Lens, Pty Ltd., Queensland, Australia) were fitted 0.10 mm flatter than the flattest k (measured with a custom-made infrared video keratometer). No ocular surface complications were observed in any marmoset in this study. Animal care, methods, and treatment protocols were all approved by the State University of New York College of Optometry Institutional Animal Care and Use Committee and were in accordance with the ARVO Statement for the Use of Animals in Ophthalmic and Vision Research.

## Refraction and Ocular Biometry Measures

Data were collected from marmosets at different stages throughout the experimental period (74 to 369 days old). On-axis cycloplegic refractive error (Nidek ARK-900 autorefractor; Nidek, Gamagori, Japan) and vitreous chamber depth (A-scan ultrasound 25 MHz; Panametrics, NDT, Ltd., Waltham, MA, USA) were measured a week prior to each ERG recording. For refractive error measurements, marmosets were awake, whereas for vitreous chamber measurements, marmosets were under anesthesia to control for eye movements (alfaxalone, 15 mg/kg, IM).

## Electroretinograms

ERGs were measured in treated and control marmosets several times throughout the experimental period (74 to 369 days old), as previously described.[32] In preparation for the ERG recordings, marmosets eyes were dilated with 1% cyclopentolate hydrochloride (Alcon, Inc., Fort Worth, TX, USA), given glycopyrrolate (0.01 mg/kg, IM) and anesthetized using acepromazine (2.5 mg/kg, IM) and ketamine (40 mg/kg, IM). Gold wire electrodes were placed on the cornea of both eyes hydrated with 0.5% carboxymethylcellulose sodium (Allergan, Inc., Madison, NJ, USA) 5 minutes after topical application of 1% proparacaine hydrochloride (Akorn, Inc., Lake Forest, IL, USA). The reference eye was covered with a black light-proof cloth. The ground probe was inserted subcutaneously in the back of the neck. The marmoset was placed over a temperature-regulated heating pad throughout the recording session and vitals were monitored every 5 minutes.

Before the stimulus presentation, marmosets were light adapted to the background light of the Espion Ganzfeld ColorDome for 10 minutes. The cone mediated ERGs were measured after a brief (200 ms) presentation of white stimuli of increasing inten-

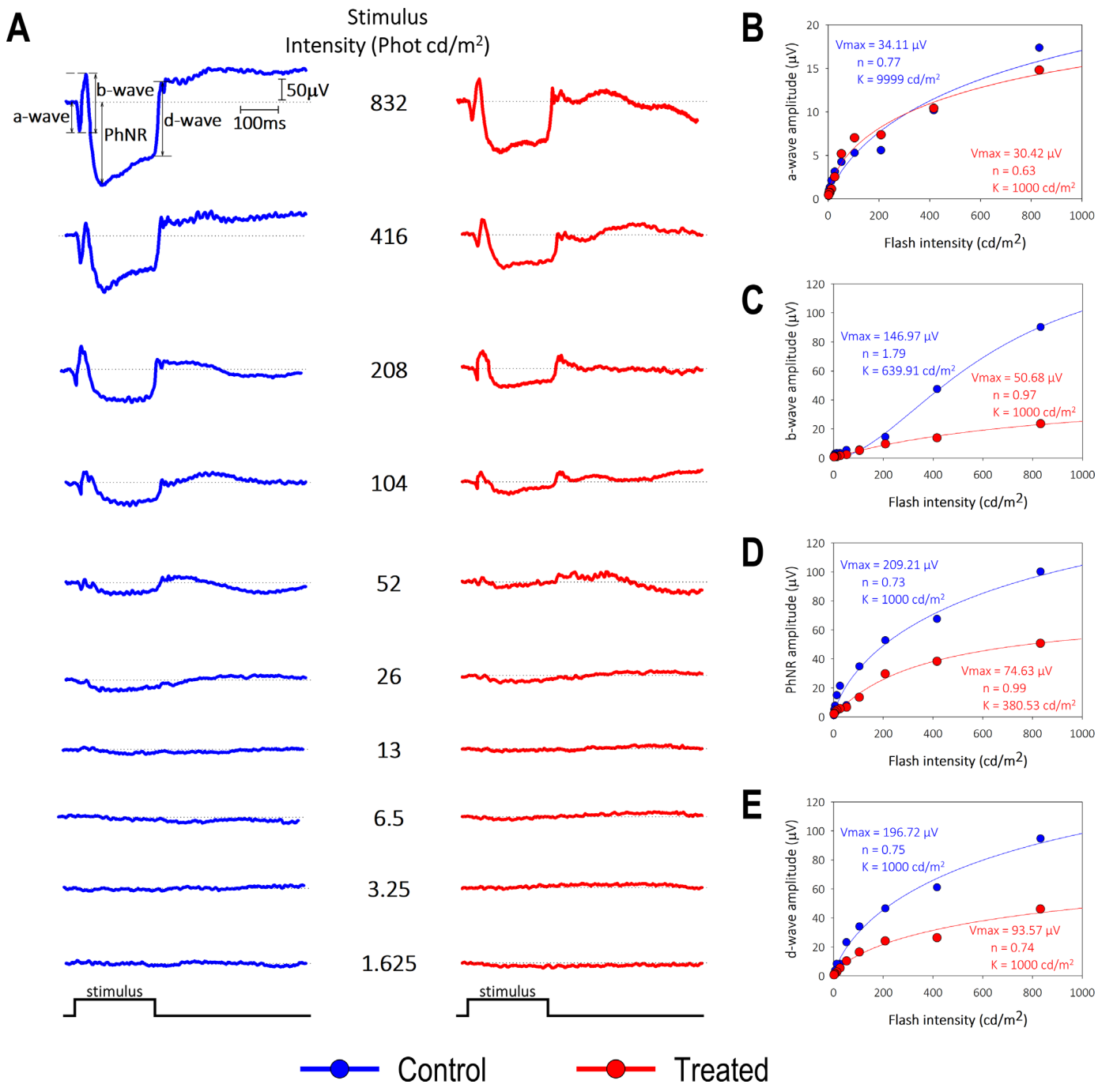


**Figure 1.** Representative photopic ERG responses and Naka-Ruston fit for a-, b-, PhNR, and d-waves. (**A**) Example of light-adapted ERG waveforms from a control marmoset (age = 77 days; Rx = 0.14 D; and VCD = 5.81 mm) and age-matched treated marmoset (age = 75 days; Rx = −0.61 D; and VCD = 5.81 mm) to 200 ms flashes of light of increasing intensities. Figure shows a-wave, b-wave, d-wave, and PhNR wave amplitude measurements. Naka-Rushton fits to the measured (**B**) a-wave, (**C**) b-wave, (**D**) PhNR wave, and (**E**) d-wave intensity-response data with the estimated values of the saturated amplitude ($V_{max}$), semi-saturation constant (K) and slope (n) for each treatment group.

sity (10 steps: 1.56-832 cd/m$^2$) on a constant white background (75 cd/m$^2$). All responses were recorded using the Espion electrodiagnostic system (Diagnosys LLC, Lowell, MA, USA). Once ERG recordings were completed, ophthalmic erythromycin ointment was applied.

The a-wave amplitude was measured from the ERG baseline to the negative a-wave trough. The b-wave amplitude was measured from the a-wave trough (or the ERG baseline if the a-wave is not present) to the b-wave peak. The d-wave was measured from light offset to the peak of the d-wave. The PhNR ampli-

tude was defined as the amplitude of the trough of the negative wave following the b-wave relative to baseline of the ERG (Fig. 1A). Stimulus intensity-response functions were plotted for the a-, b-, and d-waves, and the PhNR waves. The implicit times for all these stimulus parameters were also recorded. The intensity–response data were fitted with a generalized Naka-Rushton equation,[33] where I is the stimulus intensity, V the amplitude at intensity I, $V_{max}$ the saturated amplitude, K the semi-saturation constant (stimulus intensity at which half of the saturated amplitude is reached), and n is the slope (Figs. 1B–E).

$$V(I) = \frac{V_{max} I^n}{I^n + K^n}$$

### Statistical Analyses

Data are expressed as mean ± standard deviation (SD). Curve fitting and statistical analyses were performed using SigmaPlot (version 10.0; Systat Software, Inc., San Jose, CA, USA). The normality of the dataset was assessed using the Kolmogorov–Smirnov test. Regression analyses were used to study the relationships between refractive error/vitreous chamber depth and the ERG estimated variables. To identify how treated marmosets differed from controls, we calculated the degree of deviation from age-expected normative (AEN) data fitted regression lines for refractive error, vitreous chamber depth, a-, b-, d-, and PhNR waves. $P$ values $< 0.05$ was considered statistically significant.

## Results

### Effect of Negative Lens Treatment on Refraction and Eye Size

Marmosets treated with negative defocus developed axial myopia compared to untreated controls (refraction [Rx]: treated = −4.97 ± 4.89 diopters [D] and control = −0.97 ± 0.93 D, $P < 0.01$; vitreous chamber depth [VCD]: treated = 6.70 ± 0.60 mm and control = 6.36 ± 0.32 mm, $P < 0.05$). The change in refraction and ocular biometry with time points along with the baseline characteristics of the study marmosets are summarized in Figure 2 and the Table, respectively.

Nine marmosets (5 treated and 4 controls) had ERGs measured 7 to 14 days into treatment at similar ages (treated = 77 ± 3.39 days and control = 80.25 ± 4.99 days, $P = 0.28$), when their refraction or eye size did not yet differ (Rx: treated = −0.35 ± 1.07 D and control = −0.01 ± 0.26 D, $P = 0.56$; and VCD: treated = 5.84 ± 0.11 mm and control = 5.87 ± 0.09 mm, $P = 0.73$). When marmosets had their ERGs recorded after 4 weeks into treatment, they were more myopic and had larger eyes than controls (Rx: treated = −6.51 ± 4.69 D and control = −1.24 ± 0.86 D, $P < 0.001$; and VCD: treated = 6.99 ± 0.37 mm and control = 6.50 ± 0.21 mm, $P < 0.001$). The greater the myopia developed, the longer the vitreous chamber depths ($R^2 = 0.64$, $P < 0.001$), indicating marmosets developed axial myopia.

### Normative ERG Responses From Control Marmosets

Irrespective of age, refractive error, and vitreous chamber depth, the ERG waveforms of all control marmosets had well defined a-waves, b-waves, PhNR waves, and d-waves. There were considerable variations in the magnitude of parameters among untreated marmosets of similar age, refractive error, and VCD. As control marmosets emmetropized, there was a trend toward decreased saturated amplitudes with increasing age and normal eye growth in the PhNR, a-, b-, and d-waves. However, only the PhNR $V_{max}$ reached significance with increasing age ($R^2 = 0.29$, $P < 0.05$; Fig. 3A), emmetropization ($R^2 = 0.24$, $P < 0.05$; Fig. 3B) and normal eye growth ($R^2 = 0.42$, $P < 0.01$; Fig. 3C).

### Treated Marmosets Show Deviations From the Normative Control Dataset

There were no significant differences in PhNR $V_{max}$ (treated = −117.28 ± 31.60 µV and control = −137.02 ± 40.20 µV, $P = 0.10$), K (treated = 786.12 ± 259.21 cd/m$^2$ and control = 839.74 ± 225.80 cd/m$^2$, $P = 0.50$), n (treated = 0.84 ± 0.13 and control = 0.80 ± 0.13, $P = 0.28$), or implicit times (treated = 97.91 ± 3.19 ms and control = 97.51 ± 5.72 ms, $P = 0.80$) between treated and control marmosets when all ERG responses were averaged across time points.

However, the PhNR $V_{max}$ in treated marmosets deviated significantly from the age-norm as they got older ($R^2 = 0.58$, $P < 0.001$; Fig. 4A) and more myopic ($R^2 = 0.25$, $P < 0.05$; Fig. 4B).

There were no significant differences in the Naka-Rushton fit parameters for the b-wave between treated and control marmosets: $V_{max}$ (treated = 113.21 ± 63.85 µV and control = 115.09 ± 57.85 µV, $P = 0.93$), K (treated = 977.97 ± 79.00 cd/m$^2$ and control = 885.89 ± 235.01 cd/m$^2$, $P = 0.11$), and n (treated = 1.10 ± 0.27 and control = 1.20 ± 0.30, $P = 0.29$) at the time of ERG measurements. The b-wave implicit times were

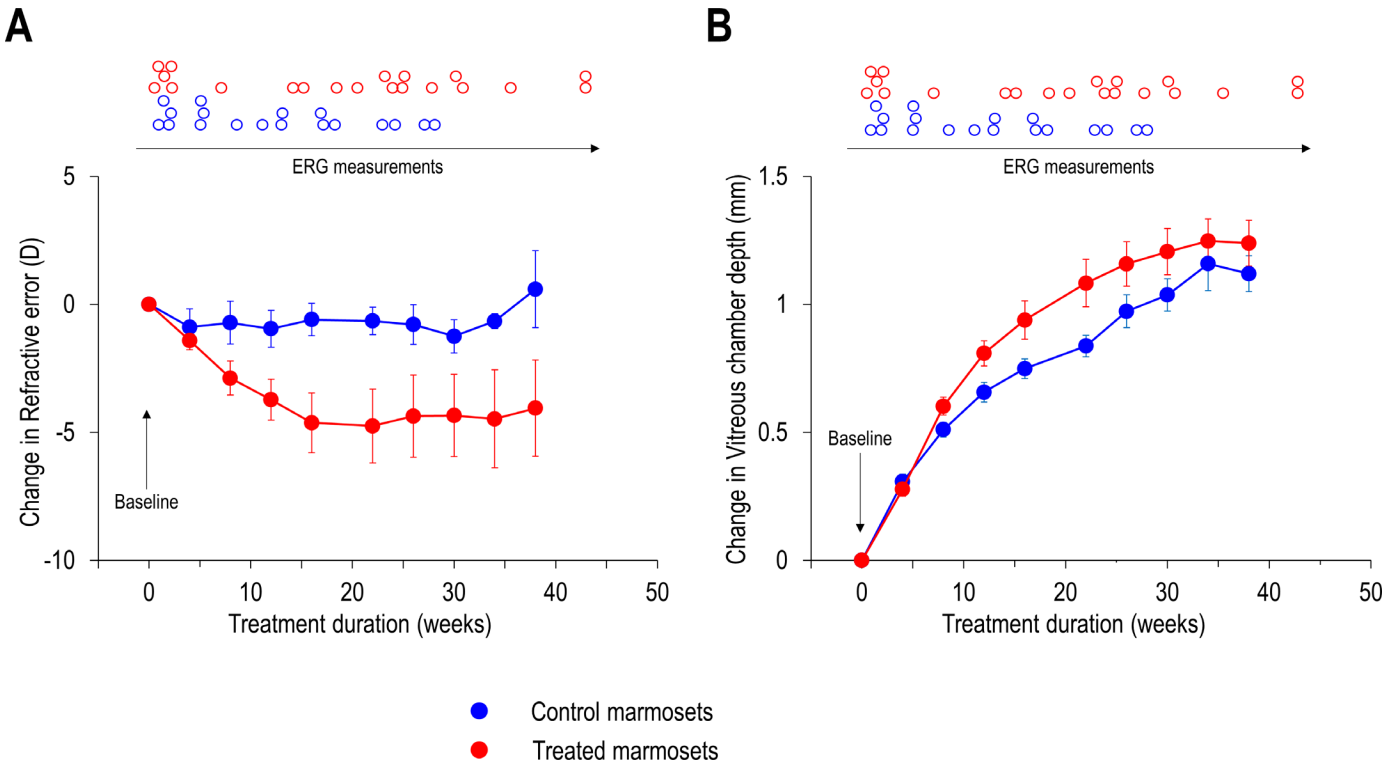


**Figure 2.** Change in (**A**) refractive error and (**B**) vitreous chamber depth, normalized to baseline, as a function of treatment duration (weeks) of negative soft contact lens treatment. *Filled circles* represent the mean for each group at timepoint during experimental period where refractive state and ocular biometry were assessed: control (*blue*) and negative-lens treated (*red*) marmosets. Positive and negative values on the ordinate represent hyperopic and myopic shift in refractive change relative to baseline, respectively. Time points of ERG recordings are denoted as *open circles* above the graph (each color represents each treatment group: control [*blue*] and negative-lens treated [*red*] marmosets). Error bars represent standard error.

**Table.** Marmoset Baseline Characteristics

| Characteristics | Treated Group | Control Group | *P* Value |
|---|---|---|---|
| *N* | 14 | 9 | |
| Sex | 5 Males, 9 Females | 7 Males, 2 Females | |
| Age (days) mean ± SD | 206 ± 98.25 | 158.44 ± 64.36 | 0.09 |
| Outcome measures at baseline, mean ± SD | | | |
| Refractive error (D) | −0.64 ± 0.76 | −0.24 ± 1.33 | 0.67 |
| Vitreous chamber depth (mm) | 5.82 ± 0.10 | 5.85 ± 0.12 | 0.39 |

also similar between the two groups (treated = 32.86 ± 2.12 ms and control = 32.26 ± 2.18 ms, $P = 0.40$). Treated marmosets showed a lower b-wave $V_{max}$ than controls at baseline that increased with increasing age ($R^2 = 0.54$, $P < 0.001$; Fig. 4C). The b-wave Naka-Rushton slope decreased significantly with increasing degrees of deviations of myopia among treated marmosets ($R^2 = 0.20$, $P < 0.05$; Fig. 4D).

The Naka-Rushton fit parameters for the d-wave as well as the implicit times at the time of ERG measurements were similar between the two groups: $V_{max}$ (treated = 97.61 ± 36.11 µV and control = 106.83 ± 47.63 µV, $P = 0.50$), K (treated = 679.46 ± 336.23 cd/m$^2$ and control = 609.42 ± 351.59 cd/m$^2$, $P = 0.53$), n (treated = 0.91 ± 0.15 and control = 0.99 ± 0.22, $P = 0.22$), implicit times (treated = 229.50 ± 1.19 ms and control = 229.43 ± 2.22 ms, $P = 0.90$). In treated marmosets, the $V_{max}$ deviations from the age-expected normative data increased with increasing age ($R^2 = 0.59$, $P < 0.001$; Fig. 4E). Similar significant

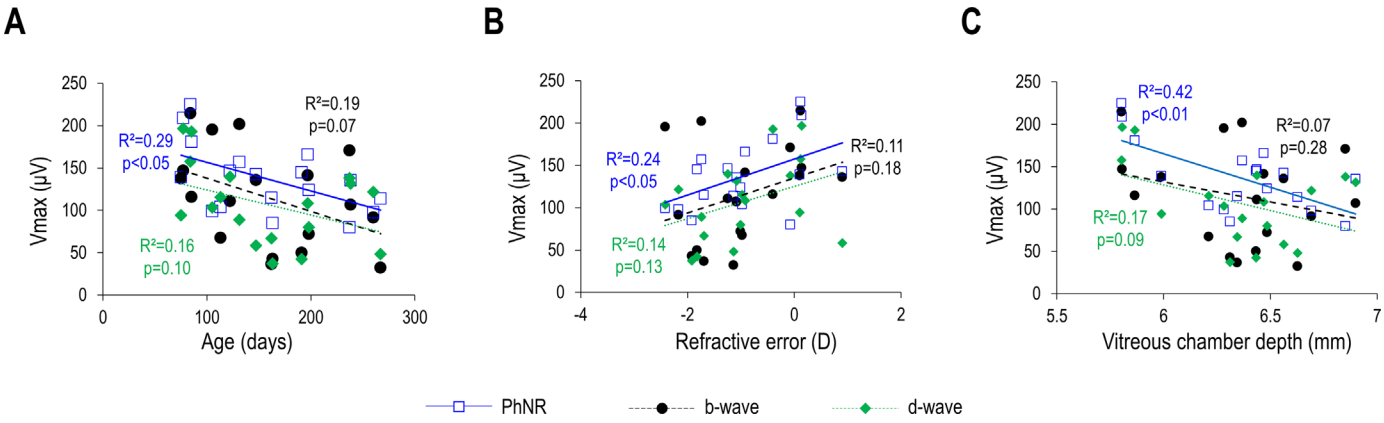


**Figure 3.** The inner retina saturated amplitude as a function of (**A**) age, (**B**) refractive error, and (**C**) vitreous chamber depth in control untreated marmosets. *Blue*, *black*, and *green symbols* and *lines* represent data and linear regression fit for the saturated amplitudes of control marmosets' PhNR wave, b-wave, and d-wave, respectively.

associations were observed for the n ($R^2 = 0.20$, $P < 0.05$; Fig. 4F) and K ($R^2 = 0.29$, $P < 0.01$; Fig. 4G) where they decreased and increased, respectively, with age.

The a-wave Naka Rushton parameters and implicit time were similar between treated and control marmosets: $V_{max}$ (treated = 44.97 ± 14.60 μV and control = 58.42 ± 19.90 μV, $P = 0.08$), K (treated = 874.11 ± 233.61 cd/m$^2$ and control = 871.14 ± 234.36 cd/m$^2$, $P = 0.98$), n (treated = 0.79 ± 0.17 and control = 0.85 ± 0.12, $P = 0.40$), and implicit times (treated = 20.21 ± 2.12 ms and control = 18.82 ± 1.71 ms, $P = 0.08$). In treated marmosets, a-wave Naka-Rushton parameters deviations from age-expected normative data were independent of age ($R^2 = 0.54$, $P = 0.31$), deviations of myopia ($R^2 = 0.04$, $P = 0.49$), and eye growth ($R^2 = 0.00$, $P = 0.82$).

Treated and control marmosets with ERGs measured 7 to 14 days into treatment showed that treatment groups at this early time point differed significantly in PhNR $V_{max}$ (treated = 100.32 ± 18.86 μV and control = 188.56 ± 37.58 μV, $P < 0.01$; Fig. 5A), b-wave $V_{max}$ (treated = 88.49 ± 22.95 μV and control = 153.82 ± 42.61 μV, $P < 0.05$; Fig. 5B), and d-wave $V_{max}$ (treated = 84.33 ± 9.01 μV and control = 160.42 ± 47.46 μV, $P < 0.01$; Fig. 5C). Treating marmosets with negative soft contact lenses for 7 to 14 days did not result in significant differences in the implicit time of the b-wave (treated = 32.94 ± 2.66 ms and control = 31.38 ± 2.06 ms, $P = 0.37$), PhNR wave (treated = 98.86 ± 3.90 ms and control = 94.25 ± 7.76 ms, $P = 0.28$), or d-wave (treated = 229.45 ± 1.27 ms and control = 228.45 ± 2.67 ms, $P = 0.48$) relative to controls. For the a-wave, the Naka-Rushton parameters and implicit time at this early time point (7–14 days into treatment) were not different between the two groups: $V_{max}$ (treated = 39.10 ± 8.67 μV and control = 57.22 ± 27.21 μV, $P = 0.19$), K (treated = 887.84 ± 250.80 cd/m$^2$ and control = 768.06 ± 282.77 cd/m$^2$, $P = 0.50$), n (treated = 0.89 ± 0.24 and control = 0.84 ± 0.15, $P = 0.70$), and implicit times (treated = 21.49 ± 2.67 ms and control = 19.86 ± 2.21 ms, $P = 0.32$).

### Relationship Among PhNR Wave, b-Wave, and d-Wave

In control animals, there was a significant association among the PhNR wave, b-wave, and d-wave, such that the PhNR wave $V_{max}$ increased as the b-wave + d-wave $V_{max}$ also increased ($R^2 = 0.31$, $P < 0.05$; Fig. 6). This relationship was not present in marmosets with induced myopia ($R^2 = 0.00$, $P = 1.00$).

## Discussion

This study provides normative ERG data from juvenile to adolescence marmosets and reports the existence of early reductions in the saturated amplitudes of the b-, d-, and PhNR wave full-field ERG responses in non-human primates with induced myopia. These saturated amplitude reductions are present before refractive and biometric changes are evident, and disappear over time as treated marmosets grow and develop myopia. The trends observed in the Naka-Rushton parameters were, in most cases, independent of refractive state and eye size in treated marmosets. The ERG implicit times were similar among marmosets, regardless of age and treatment method.

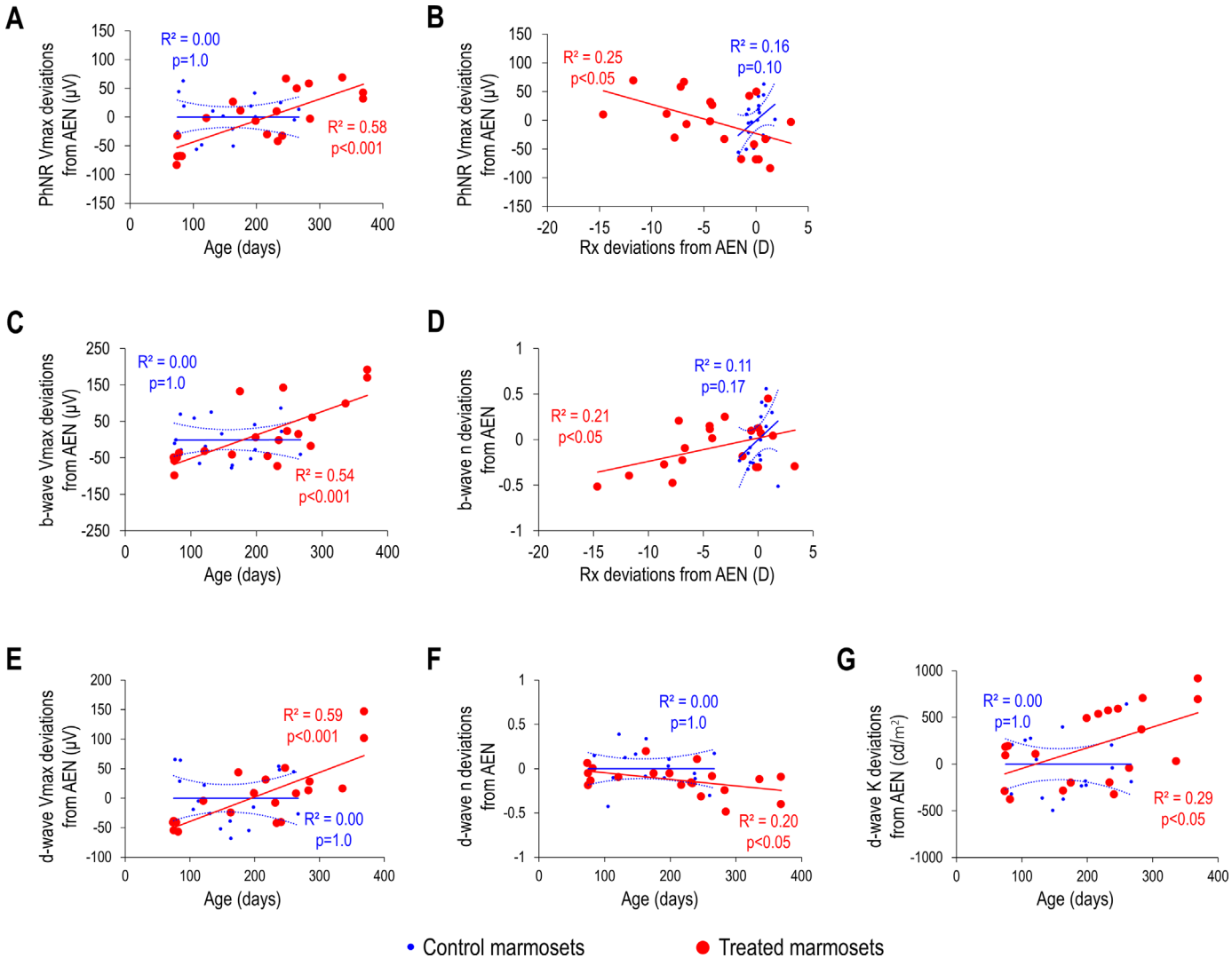


**Figure 4.** Relationship between marmoset characteristics (age and refractive error) and parameters of Naka-Rushton fits to intensity-response data of PhNR wave, b-, and d-wave. PhNR saturated amplitude ($V_{max}$) deviations from age-expected normative data (AEN) as a function of (**A**) age and (**B**) refractive error (Rx) deviations from AEN. B-wave (**C**) saturated amplitude ($V_{max}$) and (**D**) slope (n) deviations from AEN as a function of refractive error (Rx) deviations from AEN data. D-wave (**E**) saturated amplitude ($V_{max}$), (**F**) slope (n), and (**G**) semi-saturation constant (K) deviations from AEN data as a function of age. *Solid lines* represent linear regression, whereas *dotted lines* represent the upper and lower limit of 95% confidence band of the linear regression. *Blue* and *red symbols/lines* represent data/fits for control ($n = 9$) and treated ($n = 14$) marmosets, respectively.

Marmosets exposed to negative defocus for 4 weeks or longer compensated and developed axial myopia. Under this optical condition, the eye grows longer in synchrony with other ocular components and relies on visual feedback to guide compensatory changes in refraction and eye growth.[34] When the imposed defocus is removed, the eyes are myopic with an elongated vitreous chamber. This process of lens-induced myopia is present in marmosets,[31] fish,[35] birds,[36] rodents,[37,38] tree shrews,[39] and other non-human primates.[40]

The normative ERG dataset gathered from control marmosets showed that the saturated amplitude of the PhNR wave decrease with age as animals emmetropized normally. This age-related PhNR wave change in control marmosets may be attributed to postnatal retinal changes in ganglion cells and retinal glia during normal eye growth.[41,42] For instance, physiological changes known to occur, such as a decrease in the ganglion cell dendritic arbor and synaptic maturation,[43,44] postnatal naturally occurring ganglion cell apoptotic death,[45–47] large-scale natural phagocytic astrocyte cell death mediated by microglia,[48] and reduction in nerve fibers of the optic nerve in mammals,[49,50] may be present and account for the age-related reduction in the PhNR wave amplitude of

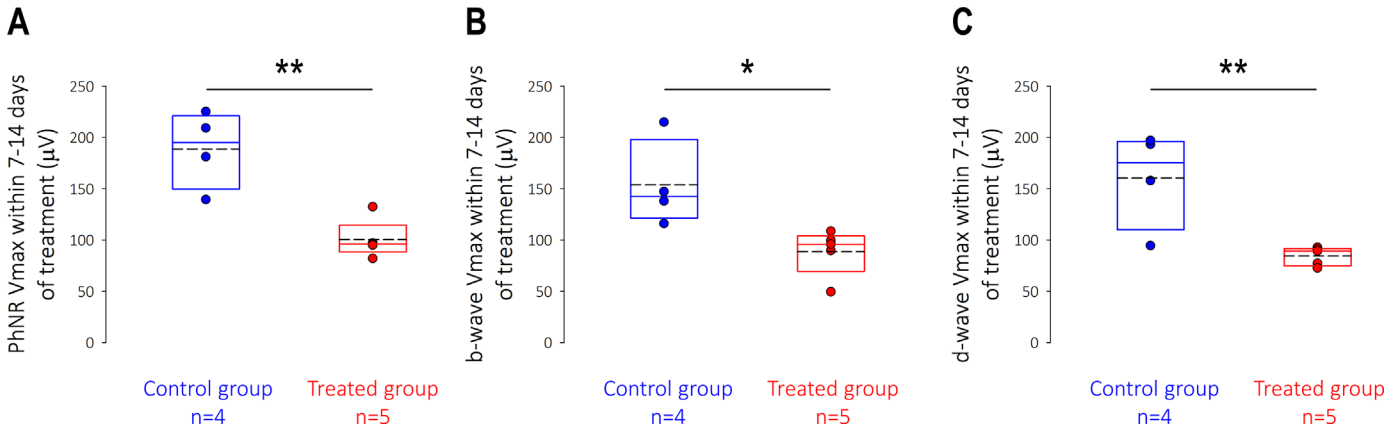


**Figure 5.** Box plots representing the summary of $V_{max}$ characteristics for the (**A**) PhNR wave, (**B**) b-wave, and (**C**) d-wave of a subset of treated (*red box*, $n = 5$) and control (*blue box*, $n = 4$) marmosets measured 7 to 14 days into treatment. The *dash line in the box* represents the mean for the respective group. Statistically significant difference between treatment groups is indicated by * $P < 0.05$ and ** $P < 0.01$.

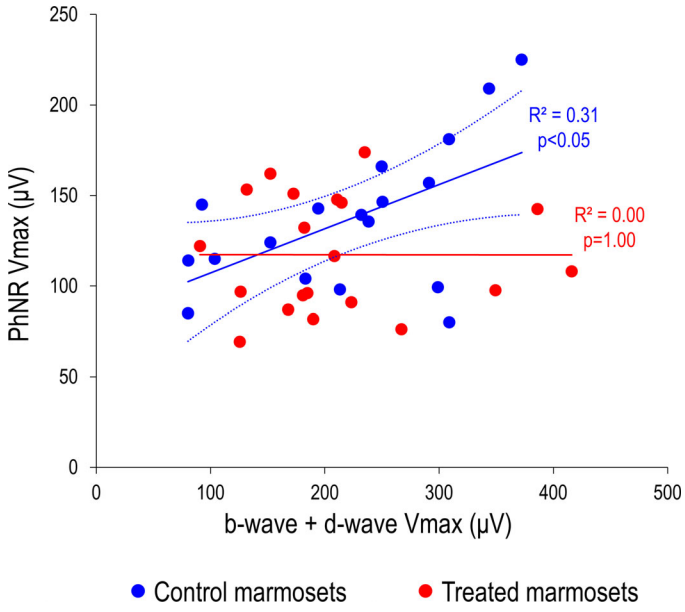


**Figure 6.** PhNR saturated amplitude ($V_{max}$) as a function of the sum of b- and d-wave saturated amplitude. *Solid lines* represent linear regression, whereas the *dotted lines* represent the upper and lower limit of 95% confidence band of the linear regression. *Blue* and *red symbols/lines* represent data/fits for control ($n = 9$) and treated ($n = 14$) marmosets, respectively.

untreated controls. The b- and d-waves exhibited a similar reduction that, however, did not reach significance. These trends may be attributed to selective programmed cell death and dynamic remodeling of synapses, known to occur after birth in photoreceptors and bipolar cells.[51,52] The absence of significance is most likely due to the normal variability in the responses, also described in children whose amplitudes also decrease with age.[53–57]

In treated marmosets, the PhNR, b-, and d-waves saturated amplitudes changed differently compared to untreated controls. Treated marmosets showed significant deviations from the age-expected normative data that increased with age. All waveform saturated responses increased as animals grew older, which was the opposite to what was seen in untreated marmosets. In human myopic eyes, there is evidence of age-related differences in the ERG response.[53,58] As suggested by Westbrook et al., changes in physical characteristics of retinal cells may be taking place as eyes develop myopia.[59]

In addition, we identified early reductions in the saturated amplitudes of the PhNR, b-, and d-waves in marmosets treated for only 7 to 14 days that disappeared over time. These early amplitude reductions have been identified in chick eyes after 3 to 4 hours of negative lens wear, and hypothesized to be due to metabolic and phototransduction changes identified using gene set enrichment analysis and occurring early during myopia development.[20] Supporting this hypothesis, retinal transcriptomes of marmosets exposed to negative defocus for 10 days versus 5 weeks have also shown an activation or suppression of largely different signaling pathways.[14] The early reductions in b- and d-waves saturated amplitudes may point to an acute attenuation of the ON-OFF responses after 7 to 14 days of imposed defocus affecting the ON-OFF retinal balance subsequently leading to the development and progression of myopia. Further, the b-wave saturated amplitude deviated significantly from the age-expected normative dataset in treated marmosets and increased as animals developed myopia. Because the b-wave is a reflection of bipolar cell activity,[16,60] this deviation from the norm may further support an ON-

OFF visual processing imbalance during myopia development.[5,7,9] These ON-OFF imbalances can occur further downstream in the visual system and not necessarily at the level of first and second order retinal neurons. Although the b-wave findings in this study are consistent with Chia et al.[61] and Luu et al.,[53] they also contradict studies reporting a reduced b-wave amplitude with increasing degrees of myopia.[55,62–64] These differences are most likely due to differences in the age of subjects and ERG protocols used (dark versus light). The unaffected semi-saturation constant (K) of the b- and d-wave responses in treated and control marmosets suggests that myopic eye growth has a minimal effect on the sensitivity of photoreceptors and bipolar cells. This, however, requires confirmation in future studies assessing the characteristics of the b- and d-waves in relation to photoreceptor and bipolar cell morphology and physiology in myopic eyes. The reduced b-wave slopes in negative-lens treated marmosets that deviated from the trend observed in untreated marmosets may suggest an altered cone ON-bipolar cell function, such as reduced luminance gain. The myopia-induced changes in the inner nuclear layer and inner plexiform layer identified in the treated marmosets may be the structural basis for this finding.[12]

The deviations in PhNR wave saturated amplitude from the normative dataset also increased as marmosets developed greater degrees of myopia. A significant correlation between the amplitude of the inner retinal response (induced component of the global-flash multifocal ERG) with increasing myopia, as well as no differences in amplitudes and implicit time between myopic and emmetropic humans have been reported by Chen et al.[65,66] This was attributed to a reduction in the inhibitory contribution to inner retina responses from reduced dopamine levels in myopes, possibly from dopaminergic amacrine cells.[11,67] In contrast, there is also evidence of reduced ganglion cell responses with increasing degrees of myopia and increasing axial length.[53,68–71] These contrasting results assessed the central and paracentral retina, whereas Chen et al.[66] and our work assessed responses from relatively larger retinal areas using a global flash system. Because the retina can respond to local defocus,[72] it is likely that global retinal responses dominated by the peripheral retina differ from macular responses. In addition, the asymmetric retinal growth experienced by myopic eyes may explain the contrasting effects of myopia on retinal responses.[73,74]

Under photopic conditions, the cone-driven a-wave parameters and implicit time did not differ between treated and control marmosets. Therefore, the differences in refractive error-driven post-photoreceptor saturated responses between treated and control marmosets appear localized to the inner retina, and possibly reflective of the altered inner retinal thickening and unaffected outer retinal thickness previously identified in myopic marmosets.[12] Although the a-wave amplitude can be similar between myopic and emmetropic young adults,[75] there is evidence of anatomic changes to photoreceptors once the myopic retina reaches a degenerative state or induces photoreceptor structural changes resulting in reduced a-wave amplitudes.[55,62,63,76,77] The unaltered a-wave implicit time indicates that the generation and speed of photoreceptors signal transmission is unaffected by physiological myopia development and progression.[55,62,75,77]

In control marmosets, the PhNR wave saturated responses increased as the b + d-wave saturated responses got larger. This trend was expected, because the b- and d-waves originate from bipolar cells and provide input to ganglion cells and feed the PhNR. In treated marmosets, however, this association was not present and the magnitude of the PhNR responses remained unchanged regardless of increases in the b- and d-waves. We have two hypotheses for the absence of this relationship in myopic animals. First, the ganglion cell complex in myopic eyes may be experiencing changes that alter ganglion cell responses. Our laboratory and others have described changes in the vascular and glial elements that support ganglion cells: reduced capillary density, increased string vessel formation, reduced astrocyte density and increased glial fibrillary acidic protein expression in marmosets,[13] microvasculature attenuation, and reduced retinal and optic nerve head blood flow in humans.[78–81] Alternatively, amacrine cells, known to modulate information from bipolar to ganglion cells and contribute to the PhNR,[24] have been suggested to be involved in myopia development and their activity might be altered.[82–85] A similar post-bipolar cell response attenuation has been suggested by Fujikado et al.[6] in form-deprived chick eyes and aligns with the hypotheses by Chui et al.[86] and Atchison et al.[87] that suggested ganglion cell dysfunction in myopic eyes due to myopic growth and tissue stretch. Because the work presented here is based on full field electrophysiology, we cannot isolate the contribution of the peripheral retina to the reduced waveform. However, studies using multifocal electroretinography have described reduced ganglion cell response amplitudes in the peripheral retina of myopes.[4,66] In addition, peripheral ganglion cells have been reported to contribute more significantly to the PhNR amplitude and are more sensitive to defects than ganglion cells in the central retina.[88,89]

Numerous studies have described a strong association between the ERG response and the degree of myopia in adult, but this relationship appears controversial in myopic children[4,53,68–71,73] In this study, we assessed the ERG responses in infant to juvenile marmosets aged 2 to 12 months approximately comparable to human childhood and early adolescence. We hypothesize that imposing negative defocus on infant marmoset eyes may trigger changes in visual perception and signal transmission that in turn result in ERG response reductions. These early adaptations may saturate over time as eyes develop myopia and match age expected control data, as suggested by retinal transcriptome findings in marmosets describing a synaptic long-term potentiation after long exposure to hyperopic defocus.[14] Alternatively, the ability to adapt to the imposed defocus may be a compensatory mechanism that is lost in older eyes, leading to a similar response in treated and control eyes at the end of treatment.

A major limitation of our study lies in our inability to establish a cause-and-effect relationship between exposure to negative lenses and the early reduction in b-, d-, and PhNR waves. This, as well as the full-field nature of the ERGs used, limits the discussion of our findings from the perspective of localized structural changes during myopia development and progression. However, this study lays the ground work for future longitudinal evaluations of the a-, b-, d-, PhNR waves, and oscillatory potential waves using both full-field and multifocal ERG measures, to study their associations with overall and localized retinal structural changes during myopia development. If pre-myopic children are confirmed to show an attenuation of the b-, d-, and PhNR waves before refractive and ocular biometric changes are evident, these ERG parameters may become valuable early clinical markers to help identify children at risk of developing myopia, and facilitate access to early myopia control interventions to delay the onset of associated ocular complications.

In summary, this study provides evidence of an early reduction in the saturated amplitudes of the b-, d-, and PhNR waves in negative-lens treated marmosets compared to controls. In addition, the relationship between ganglion cell activity and its bipolar cell inputs observed in untreated eyes was not present in myopic eyes. These electrophysiology findings confirm the dynamic nature of the cell function in myopia development and progression, and suggest the existence of early visual processing and cell physiology changes taking place in eyes with myopia.

## Acknowledgments

Supported by The American Academy of Optometry Career Development Award to Alexandra Benavente-Perez. The authors are immensely grateful to Suresh Viswanathan for his help with electroretinogram recordings, data analysis, and interpretation. We further thank Gulnoza Azieva, Stephanie Liang, Christina Canellos, Peter Yoon, Stephen Dellostritto, Amy Pope, and Hardy Zhou for their assistance with lens insertion and removal. We are also grateful to Ann Nour, Catherine Suarez, and Jibin Zachariah for their help with data collection, and the Biological Research Facility at SUNY College of Optometry for their assistance with animal care.

Disclosure: **R.K. Ablordeppey**, None; **R. Nieu**, None; **C.R. Lin**, None; **A. Benavente-Perez**, None

## References

1. Wallman J, Winawer J. Homeostasis of eye growth and the question of myopia. *Neuron*. 2004;43(4):447–468.
2. Saw SM, Gazzard G, Shih-Yen EC, Chua WH. Myopia and associated pathological complications. *Ophthalmic Physiol Opt*. 2005;25(5):381–391.
3. Troilo D, Gottlieb MD, Wallman J. Visual deprivation causes myopia in chicks with optic nerve section. *Curr Eye Res*. 1987;6(8):993–999.
4. Kawabata H, Adachi-Usami E. Multifocal electroretinogram in myopia. *Invest Ophthalmol Vis Sci*. 1997;38(13):2844–2851.
5. Chakraborty R, Park HN, Hanif AM, Sidhu CS, Iuvone PM, Pardue MT. ON pathway mutations increase susceptibility to form-deprivation myopia. *Exp Eye Res*. 2015;137:79–83.
6. Fujikado T, Hosohata J, Omoto T. ERG of form deprivation myopia and drug induced ametropia in chicks. *Curr Eye Res*. 1996;15(1):79–86.
7. Pardue MT, Faulkner AE, Fernandes A, et al. High susceptibility to experimental myopia in a mouse model with a retinal on pathway defect. *Invest Ophthalmol Vis Sci*. 2008;49(2):706–712.
8. Smith EL, 3rd, Fox DA, Duncan GC. Refractive-error changes in kitten eyes produced by chronic on-channel blockade. *Vision Res*. 1991;31(5):833–844.
9. Wang M, Aleman AC, Schaeffel F. Probing the potency of artificial dynamic ON or OFF stimuli

to inhibit myopia development. *Invest Ophthalmol Vis Sci*. 2019;60(7):2599–2611.
10. Aleman AC, Wang M, Schaeffel F. Reading and myopia: contrast polarity matters. *Sci Rep*. 2018;8(1):10840.
11. Stone RA, Lin T, Laties AM, Iuvone PM. Retinal dopamine and form-deprivation myopia. *Proc Natl Acad Sci USA*. 1989;86(2):704–706.
12. Ablordeppey RK, Lin C, Benavente-Perez A. The age-related pattern of inner retinal thickening is affected by myopia development and progression. *Sci Rep*. 2022;12(1):22190.
13. Lin C, Toychiev A, Ablordeppey R, Slavi N, Srinivas M, Benavente-Perez A. Myopia alters the structural organization of the retinal vasculature, GFAP-positive glia, and ganglion cell layer thickness. *Int J Mol Sci*. 2022;23(11):6202.
14. Tkatchenko TV, Troilo D, Benavente-Perez A, Tkatchenko AV. Gene expression in response to optical defocus of opposite signs reveals bidirectional mechanism of visually guided eye growth. *PLoS Biol*. 2018;16(10):e2006021.
15. Bush RA, Sieving PA. A proximal retinal component in the primate photopic ERG a-wave. *Invest Ophthalmol Vis Sci*. 1994;35(2):635–645.
16. Stockton RA, Slaughter MM. B-wave of the electroretinogram. A reflection of ON bipolar cell activity. *J Gen Physiol*. 1989;93(1):101–122.
17. Szikra T, Witkovsky P. Contributions of AMPA- and kainate-sensitive receptors to the photopic electroretinogram of the Xenopus retina. *Vis Neurosci*. 2001;18(2):187–196.
18. Gupta SK, Chakraborty R, Verkicharla PK. Electroretinogram responses in myopia: a review. *Doc Ophthalmol*. 2022;145(2):77–95.
19. Zahra S, Murphy MJ, Crewther SG, Riddell N. Flash electroretinography as a measure of retinal function in myopia and hyperopia: a systematic review. *Vision (Basel)*. 2023;7(1):15.
20. Riddell N, Murphy MJ, Crewther SG. Electroretinography and gene expression measures implicate phototransduction and metabolic shifts in chick myopia and hyperopia models. *Life*. 2021;11(6):501.
21. Jiang X, Xu Z, Soorma T, et al. Electrical responses from human retinal cone pathways associate with a common genetic polymorphism implicated in myopia. *Proc Natl Acad Sci USA*. 2022;119(21):e2119675119.
22. Thompson DA, Feather S, Stanescu HC, et al. Altered electroretinograms in patients with KCNJ10 mutations and EAST syndrome. *J Physiol*. 2011;589(Pt 7):1681–1689.
23. Kumar S, Benavente-Perez A, Ablordeppey R, et al. A robust microbead occlusion model of glaucoma for the common marmoset. *Transl Vis Sci Technol*. 2022;11(1):14.
24. Viswanathan S, Frishman LJ, Robson JG, Harwerth RS, Smith EL, 3rd. The photopic negative response of the macaque electroretinogram: reduction by experimental glaucoma. *Invest Ophthalmol Vis Sci*. 1999;40(6):1124–1136.
25. Viswanathan S, Frishman LJ, Robson JG, Walters JW. The photopic negative response of the flash electroretinogram in primary open angle glaucoma. *Invest Ophthalmol Vis Sci*. 2001;42(2):514–522.
26. Machida S, Raz-Prag D, Fariss RN, Sieving PA, Bush RA. Photopic ERG negative response from amacrine cell signaling in RCS rat retinal degeneration. *Invest Ophthalmol Vis Sci*. 2008;49(1):442–452.
27. Miyata K, Nakamura M, Kondo M, et al. Reduction of oscillatory potentials and photopic negative response in patients with autosomal dominant optic atrophy with OPA1 mutations. *Invest Ophthalmol Vis Sci*. 2007;48(2):820–824.
28. Chen H, Zhang M, Huang S, Wu D. The photopic negative response of flash ERG in nonproliferative diabetic retinopathy. *Doc Ophthalmol*. 2008;117(2):129–135.
29. Machida S, Gotoh Y, Tanaka M, Tazawa Y. Predominant loss of the photopic negative response in central retinal artery occlusion. *Am J Ophthalmol*. 2004;137(5):938–940.
30. Benavente-Perez A, Nour A, Troilo D. The effect of simultaneous negative and positive defocus on eye growth and development of refractive state in marmosets. *Invest Ophthalmol Vis Sci*. 2012;53(10):6479–6487.
31. Benavente-Pérez A, Nour A, Troilo D. Axial eye growth and refractive error development can be modified by exposing the peripheral retina to relative myopic or hyperopic defocus. *Invest Ophthalmol Vis Sci*. 2014;55(10):6765–6773.
32. Ablordeppey RK, Lin CR, Song B, Benavente-Perez A. Choroidal morphology and photoreceptor activity are related and affected by myopia development. *Invest Ophthalmol Vis Sci*. 2024;65(2):3.
33. Severns ML, Johnson MA. The care and fitting of Naka-Rushton functions to electroretinographic intensity-response data. *Doc Ophthalmol*. 1993;85(2):135–150.
34. Schaeffel F, Glasser A, Howland HC. Accommodation, refractive error and eye growth in chickens. *Vision Res*. 1988;28(5):639–657.

35. Shen W, Sivak JG. Eyes of a lower vertebrate are susceptible to the visual environment. *Invest Ophthalmol Vis Sci*. 2007;48(10):4829–4837.
36. Schaeffel F, Troilo D, Wallman J, Howland HC. Developing eyes that lack accommodation grow to compensate for imposed defocus. *Vis Neurosci*. 2009;4(2):177–183.
37. Howlett MHC, McFadden SA. Spectacle lens compensation in the pigmented guinea pig. *Vision Res*. 2009;49(2):219–227.
38. Jiang X, Kurihara T, Kunimi H, et al. A highly efficient murine model of experimental myopia. *Sci Rep*. 2018;8(1):2026.
39. Siegwart JT, Jr., Norton TT. Binocular lens treatment in tree shrews: effect of age and comparison of plus lens wear with recovery from minus lens-induced myopia. *Exp Eye Res*. 2010;91(5):660–669.
40. Smith EL, 3rd, Hung LF. The role of optical defocus in regulating refractive development in infant monkeys. *Vision Res*. 1999;39(8):1415–1435.
41. Hendrickson A, Troilo D, Possin D, Springer A. Development of the neural retina and its vasculature in the marmoset Callithrix jacchus. *J Comp Neurol*. 2006;497(2):270–286.
42. Kuhrt H, Gryga M, Wolburg H, et al. Postnatal mammalian retinal development: quantitative data and general rules. *Prog Retin Eye Res*. 2012;31(6):605–621.
43. Samuel MA, Zhang Y, Meister M, Sanes JR. Age-related alterations in neurons of the mouse retina. *J Neurosci*. 2011;31(44):16033–16044.
44. Sandalon S, Ofri R. Age-related changes in the pattern electroretinogram of normal and glatiramer acetate–immunized rats. *Invest Ophthalmol Vis Sci*. 2012;53(10):6532–6540.
45. Potts RA, Dreher B, Bennett MR. The loss of ganglion cells in the developing retina of the rat. *Brain Res*. 1982;255(3):481–486.
46. Lipton SA. Blockade of electrical activity promotes the death of mammalian retinal ganglion cells in culture. *Proc Natl Acad Sci USA*. 1986;83(24):9774–9778.
47. Williams MA, Piñon LG, Linden R, Pinto LH. The pearl mutation accelerates the schedule of natural cell death in the early postnatal retina. *Exp Brain Res*. 1990;82(2):393–400.
48. Puñal VM, Paisley CE, Brecha FS, et al. Large-scale death of retinal astrocytes during normal development is non-apoptotic and implemented by microglia. *PLoS Biol*. 2019;17(10):e3000492.
49. Balazsi AG, Rootman J, Drance SM, Schulzer M, Douglas GR. The effect of age on the nerve fiber population of the human optic nerve. *Am J Ophthalmol*. 1984;97(6):760–766.
50. Johnson BM, Miao M, Sadun AA. Age-related decline of human optic nerve axon populations. *AGE*. 1987;10(1):5–9.
51. Péquignot MO, Provost AC, Sallé S, et al. Major role of BAX in apoptosis during retinal development and in establishment of a functional postnatal retina. *Dev Dyn*. 2003;228(2):231–238.
52. West ER, Cepko CL. Development and diversification of bipolar interneurons in the mammalian retina. *Dev Biol*. 2022;481:30–42.
53. Luu CD, Lau AMI, Lee S-Y. Multifocal electroretinogram in adults and children with myopia. *Arch Ophthalmol*. 2006;124(3):328–334.
54. Peterson H. The normal B-potential in the single-flash clinical electroretinogram. A computer technique study of the influence of sex and age. *Acta Ophthalmol*. 1968:99(Suppl):97–77.
55. Westall CA, Dhaliwal HS, Panton CM, et al. Values of electroretinogram responses according to axial length. *Doc Ophthalmol*. 2001;102(2):115–130.
56. Birch DG, Anderson JL. Standardized full-field electroretinography. Normal values and their variation with age. *Arch Ophthalmol*. 1992;110(11):1571–1576.
57. Brecelj J, Strucl M, Zidar I, Tekavcic-Pompe M. Pattern ERG and VEP maturation in schoolchildren. *Clin Neurophysiol*. 2002;113(11):1764–1770.
58. Charng J, Nguyen CTO, Bui BV, Vingrys AJ. Age-related retinal function changes in albino and pigmented rats. *Invest Ophthalmol Vis Sci*. 2011;52(12):8891–8899.
59. Westbrook AM, Crewther DP, Crewther SG. Cone receptor sensitivity is altered in form deprivation myopia in the chicken. *Optom Vis Sci*. 1999;76(5):326–338.
60. Xu X, Karwoski C. Current source density analysis of the electroretinographic d wave of frog retina. *J Neurophysiol*. 1995;73(6):2459–2469.
61. Chia A, Li W, Tan D, Luu CD. Full-field electroretinogram findings in children in the atropine treatment for myopia (ATOM2) study. *Doc Ophthalmol*. 2013;126(3):177–186.
62. Perlman I, Meyer E, Haim T, Zonis S. Retinal function in high refractive error assessed electroretinographically. *Br J Ophthalmol*. 1984;68(2):79–84.
63. Flitcroft DI, Adams GG, Robson AG, Holder GE. Retinal dysfunction and refractive errors: an electrophysiological study of children. *Br J Ophthalmol*. 2005;89(4):484–488.
64. Kader MA. Electrophysiological study of myopia. *Saudi J Ophthalmol*. 2012;26(1):91–99.

65. Chen JC, Brown B, Schmid KL. Delayed mfERG responses in myopia. *Vision Res*. 2006;46(8):1221–1229.
66. Chen JC, Brown B, Schmid KL. Retinal adaptation responses revealed by global flash multifocal electroretinogram are dependent on the degree of myopic refractive error. *Vision Res*. 2006;46(20):3413–3421.
67. Guo SS, Sivak JG, Callender MG, Diehl-Jones B. Retinal dopamine and lens-induced refractive errors in chicks. *Curr Eye Res*. 1995;14(5):385–389.
68. Hidajat R, McLay J, Burley C, Elder M, Morton J, Goode D. Influence of axial length of normal eyes on PERG. *Doc Ophthalmol*. 2003;107(2):195–200.
69. Li SZ, Yu WY, Choi KY, et al. Subclinical decrease in central inner retinal activity is associated with myopia development in children. *Invest Ophthalmol Vis Sci*. 2017;58(10):4399–4406.
70. Ho W-C, Kee C-S, Chan HH-L. Myopic children have central reduction in high contrast multifocal ERG response, while adults have paracentral reduction in low contrast response. *Invest Ophthalmol Vis Sci*. 2012;53(7):3695–3702.
71. W-c Ho, C-s Kee, HH-l Chan. Myopia progression in children is linked with reduced foveal mfERG response. *Invest Ophthalmol Vis Sci*. 2012;53(9):5320–5325.
72. Ho WC, Wong OY, Chan YC, Wong SW, Kee CS, Chan HH. Sign-dependent changes in retinal electrical activity with positive and negative defocus in the human eye. *Vision Res*. 2012;52(1):47–53.
73. Koh V, Tan C, Nah G, et al. Correlation of structural and electrophysiological changes in the retina of young high myopes. *Ophthalmic Physiol Opt*. 2014;34(6):658–666.
74. Wolsley CJ, Saunders KJ, Silvestri G, Anderson RS. Investigation of changes in the myopic retina using multifocal electroretinograms, optical coherence tomography and peripheral resolution acuity. *Vision Res*. 2008;48(14):1554–1561.
75. Wan W, Chen Z, Lei B. Increase in electroretinogram rod-driven peak frequency of oscillatory potentials and dark-adapted responses in a cohort of myopia patients. *Doc Ophthalmol*. 2020;140(2):189–199.
76. Blach RK, Jay B, Kolb H. Electrical activity of the eye in high myopia. *Br J Ophthalmol*. 1966;50(11):629–641.
77. Sachidanandam R, Ravi P, Sen P. Effect of axial length on full-field and multifocal electroretinograms. *Clin Exp Optom*. 2017;100(6):668–675.
78. Benavente-Pérez A, Hosking SL, Logan NS, Broadway DC. Ocular blood flow measurements in healthy human myopic eyes. *Graefes Arch Clin Exp Ophthalmol*. 2010;248(11):1587–1594.
79. Lim LS, Cheung CY, Lin X, Mitchell P, Wong TY, Mei-Saw S. Influence of refractive error and axial length on retinal vessel geometric characteristics. *Invest Ophthalmol Vis Sci*. 2011;52(2):669–678.
80. Shimada N, Ohno-Matsui K, Harino S, et al. Reduction of retinal blood flow in high myopia. *Graefes Arch Clin Exp Ophthalmol*. 2004;242(4):284–288.
81. Benavente-Perez A. Evidence of vascular involvement in myopia: a review. *Front Med*. 2023;10:1112996.
82. Schmid KL, Strasberg G, Rayner CL, Hartfield PJ. The effects and interactions of GABAergic and dopaminergic agents in the prevention of form deprivation myopia by brief periods of normal vision. *Exp Eye Res*. 2013;110:88–95.
83. Ashby R, Kozulin P, Megaw PL, Morgan IG. Alterations in ZENK and glucagon RNA transcript expression during increased ocular growth in chickens. *Mol Vis*. 2010;16:639–649.
84. Yao Y, Chen Z, Wu Q, Lu Y, Zhou X, Zhu X. Single-cell RNA sequencing of retina revealed novel transcriptional landscape in high myopia and underlying cell-type-specific mechanisms. *MedComm (2020)*. 2023;4(5):e372.
85. Banerjee S, Wang Q, Zhao F, et al. Increased connexin36 phosphorylation in AII amacrine cell coupling of the mouse myopic retina. *Front Cell Neurosci*. 2020;14:124.
86. Chui TY, Yap MK, Chan HH, Thibos LN. Retinal stretching limits peripheral visual acuity in myopia. *Vision Res*. 2005;45(5):593–605.
87. Atchison DA, Schmid KL, Pritchard N. Neural and optical limits to visual performance in myopia. *Vision Res*. 2006;46(21):3707–3722.
88. Morny EKA, Patel K, Votruba M, Binns AM, Margrain TH. The relationship between the photopic negative response and retinal ganglion cell topography. *Invest Ophthalmol Vis Sci*. 2019;60(6):1879–1887.
89. Tamada K, Machida S, Yokoyama D, Kurosaka D. Photopic negative response of full-field and focal macular electroretinograms in patients with optic nerve atrophy. *Jpn J Ophthalmol*. 2009;53(6):608–614.